

Peak seismic response of a symmetric base-isolated steel building: near vs. far fault excitations and varying incident angle

Constantina Pavlidou and Petros Komodromos*

Department of Civil & Environmental Engineering, School of Engineering, University of Cyprus, Nicosia, Cyprus

(Received September 22, 2019, Revised December 23, 2019, Accepted December 30, 2019)

Abstract. Since the peak seismic response of a base-isolated building strongly depends on the characteristics of the imposed seismic ground motion, the behavior of a base-isolated building under different seismic ground motions is studied, in order to better assess their effects on its peak seismic response. Specifically, the behavior of a typical steel building is examined as base-isolated with elastomeric bearings, while the effect of near-fault ground motions is studied by imposing 7 pairs of near- and 7 pairs of far-fault seismic records, from the same 7 earthquake events, to the building, under 3 different loading combinations, through three-dimensional (3D) nonlinear dynamic analyses, conducted with SAP2000. The results indicate that near-fault seismic components are more likely to increase the building's peak seismic response than the corresponding far-fault components. Furthermore, the direction of the imposed earthquake excitations is also varied by rotating the imposed pairs of seismic records from 0° to 360°, with respect to the major construction axes. It is observed that the peak seismic responses along the critical incident angles, which in general differ from the major horizontal construction axes of the building, are significantly higher. Moreover, the influence of 5% and 10% accidental mass eccentricities is also studied, revealing that when considering accidental mass eccentricities the peak relative displacements of the base isolated building at the isolation level are substantially increased, while the peak floor accelerations and interstory drifts of its superstructure are only slightly affected.

Keywords: base isolation; seismic isolation; peak seismic response; near vs. far fault; incident angle

1. Introduction

During the last decades, seismic isolation has been established as an effective earthquake resistant design approach, by avoiding resonance with the predominant frequencies of strong earthquakes in order to reduce the induced seismic loads. It is evident that the peak seismic response of a base-isolated building strongly depends not only on the superstructure's and the seismic isolation system's characteristics, but also on the characteristics of the imposed seismic ground motion. Thus, it would be very important to study the seismic behavior of base-isolated buildings subjected to different types of earthquake excitations and under various seismic incident angles, in order to better assess their influences on the effectiveness of seismic isolation in reducing its peak seismic response.

Although considerable reductions of both interstory drifts and peak floor accelerations can be achieved by seismic isolation, during strong seismic excitations, very large relative displacements are expected, at the isolation level, which is usually at a level between the ground and the superstructure. Therefore, it is very critical to reliably assess the maximum expected relative displacements in order to provide a sufficiently wide seismic gap around a seismically isolated building to enable unobstructed movements of the

superstructure and prevent potential structural pounding with adjacent structures and the surrounding moat wall during very strong earthquakes.

The peak seismic response of a base-isolated structure depends on the seismic activity of the region and the intensity and characteristics of the earthquake excitations. It has been observed that the recorded seismic ground motions at stations located near the fault have certain differences from the ground motions recorded at stations at longer distances. A near-fault (NF) ground motion can be defined by the distance between the rupture and the recordings, of about 20km (Bray *et al.*, 2004). Seismic ground motions occurred in the NF area, are affected by the rupture mechanism, the rupture directivity with respect to the area and possible permanent ground displacements because of the sliding of the rupture. Seismologists have identified (a) large amplitude and long periods, (b) high PGV/PGA and PGD/PGA ratios, (c) unusual response spectra shapes and (d) significant energy being contained in the first few pulses, as the main characteristics of NF ground motions.

Specifically, Kramer *et al.* (1996) pointed out that forward-directivity effects, where the rupture propagates to the area of the building, can enhance vibration pulses, especially when the rupture propagation velocity equals the velocity of the seismic motions, which cause significant relative displacements. Earthquakes with predominant frequencies close to the fundamental eigenfrequencies of buildings may cause significant damage due to resonance, which amplifies the response. However, NF ground motions with large magnitudes cannot all be assumed as the "worst-

*Corresponding author, Professor
E-mail: komodromos@ucy.ac.cy

case scenarios” for the design of all buildings. For example, Mavroeidis *et al.* (2004) implemented simple mathematical models for the characterization and parameterization of the near-fault strong ground motions and highlighted that the duration of the near-fault ground motion pulse was the most determining parameter in the elastic and inelastic performance of a SDOF system. Furthermore, it was pointed out that the impulsive character of the NF velocity pulse affects significantly the elastic response spectra of the SDOF system. Additionally, Bray *et al.* (2004) mentioned that most of the energy in forward-directivity ground motions is concentrated on the narrow-period band centered on the pulse period. Consequently, lower magnitude events might produce more damaging ground motions for stiff buildings, which are far more common in urban areas. Moreover, Zhang *et al.* (2013) performed seismic damage analyses, which showed that accumulated damage of concrete gravity dams was significantly affected by NF ground motions. In particular, it was observed that the nonlinear response obtained from NF ground motions had a considerably different and greater displacement history than those obtained from far-fault (FF) ground motions.

Regarding the effect of the incident angle of a seismic ground motion, several studies have shown that it significantly affects the peak seismic response of a building. For example, Athanatopoulou (2005) performed linear time-history analyses under several earthquake records and different incident angles, showing that the critical value of a response quantity could be up to 80% larger than the corresponding peak values when the seismic components are applied along the major construction axes of the building. Moreover, Kostinakis *et al.* (2015) revealed that when different incident angles are considered, the majority of intensity measures show medium correlation with the overall structural damage index in case of the frame systems, whereas no certain seismic intensity measure seems to be the most reliable. Rigato *et al.* (2007), demonstrated that the peak inelastic deformation demands are underestimated because they often occur when the ground motion is applied at orientations other than the principal construction axes of the building, regardless of whether there is a torsional irregularity in the building or not (Kostinakis *et al.* (2012), Nguyen and Kim (2013)). Also, the results demonstrated that the incident angle should be taken into account in earthquake design, although this has not yet been included in the building codes. Additionally, Kostinakis *et al.* (2015), by performing nonlinear time response analyses, revealed that the damage level of the buildings examined was strongly affected by the incident angle of the imposed ground motion, even in double-symmetric in plan buildings. Hence, when applying the earthquake records solely along the structural axes, might lead to significant underestimation of structural damage. Furthermore, in the same paper, it was observed that NF ground motions caused worse damage to the structures than the FF records. It should be noted that several parametric studies regarding the influence of the incident angle on the structural response, show that it is difficult to define the critical angle (Magliulo *et al.* (2014), Lagaros *et al.* (2010a), Reyes and Kalkan (2015), Fontara *et*

al. (2015)). Moreover, research studies have shown that the critical incident angle is influenced more by the characteristics of the excitation, rather than by the properties of the building (Kalkan *et al.* 2014). Therefore, it would be difficult to determine an optimal building orientation that maximizes the demands of a building before performing time-history analyses.

According to the above, the importance of taking into account seismic ground motions in directions other than the major structural axes of the building during the seismic design, in order to more reliably assess their peak seismic responses considering the worst-case scenario, is highlighted.

In this research work, the behavior of a typical base-isolated steel building is examined for different load combinations and under various seismic ground motions. Three-dimensional (3D), nonlinear inelastic, time-history analyses are conducted, using the SAP2000 software, in order to take into account the nonlinear behavior of the base isolation system, while the superstructure is considered to have linear response, and considering different structural and seismic characteristics. More precisely, the behavior of the symmetric base-isolated model without and with mass eccentricities is examined, while the direction of the imposed earthquake excitations is varied as well. Specifically, the peak seismic response of a typical base-isolated steel building supported on a combination of lead-rubber bearings (LRBs) and natural-rubber bearings (NRBs) is investigated, in an effort to better understand the effect of the various parameters that control the peak seismic behavior of such seismically isolated structures. Particularly, the effect of NF ground motions, the effect of the incident angle, as well as the effect of accidental mass eccentricities are investigated. In order to study the effect of NF ground motions, different types of seismic records are imposed to the simulated building, while the direction of the imposed earthquake excitations is also varied by rotating the seismic record pairs from 0° to 360°, with a 15° interval with respect to the major construction axes so as to examine the influence of incident angles that are different from the two major horizontal construction axes of the building. Subsequently, the influence of accidental mass eccentricities is also studied according to relevant provisions in seismic design regulations.

2. Design and modeling assumptions

2.1 Superstructure

The spatial (3D) model of a typical steel building examined was initially designed and studied by Varnava *et al.* (2013). The structure is a two-story building with plan dimensions 24 m x 20 m and floor heights of 3.30 m. The frame in the X direction has 3 equal spans of 8 m each, while the frame in the Y direction has 4 spans of 5 m each. A moment resisting frame is designed in the X direction, with rigidly connected beams to the columns, while the frames in the Y direction act like trusses: the beam-column connection is pin-jointed, while the edge sides of the outer

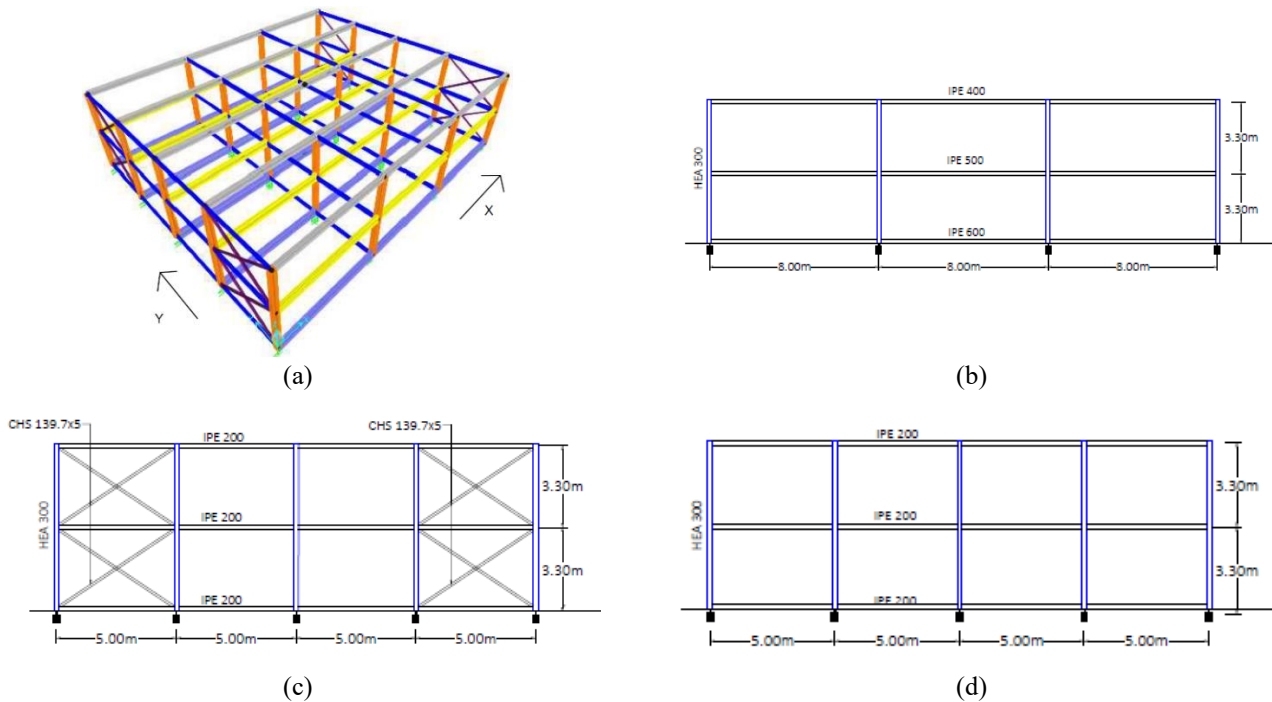


Fig. 1 (a) 3D view of the base-isolated building, with respect to the horizontal construction axes, X and Y (b) Cross section of a frame in the primary direction shown in the XZ plane (c) Cross section of an external frame in the secondary direction shown in the YZ plane (d) Cross section of an internal frame in the secondary direction shown in the YZ plane

frames are concentrically braced. A 3D view of the considered base-isolated building is shown in Fig. 1, as well as the cross sections of the three types of frames. Each floor is simulated as a rigid diaphragm and the masses are lumped at the floor levels.

2.2 Design and modeling of the NRBs and LRBs

The design of the base isolation system was conducted by Varnava *et al.* (2013), by selecting a target eigenperiod $T_{dur}=1.2\text{sec}$. More, precisely, the computed eigenperiods and the corresponding effective modal masses participation factors are presented in Table 1. The corresponding acceleration of the design spectrum $S_d(1.2)$ equals $0.3125g$. Both NRBs and LRBs are defined as "Rubber Isolator" type link elements in the SAP2000 structural analysis software. The NRBs have been modeled assuming equivalent (or effective) linear properties, while nonlinear inelastic properties have been used for modeling the LRBs. The mechanical characteristics of the isolators are given in Table 2.

The minimum required width of the seismic gap, according to two different regulations, is calculated in order to compare it with the corresponding value as computed by the conducted dynamic analyses. Specifically, the seismic gap based on the EC8 provisions is calculated by Eq. (1), in which D_d is an approximate calculation of the displacement of the system at the isolation level and δ_{xi}, δ_{yi} are the magnification coefficients in the X and Y direction, respectively. As noted in EC8, for a better reliability, the required displacements should be multiplied by the magnification factor γ_x , which, according to Cyprus

National Appendix CYS EN 1998-1: 2004, is set to 1.2.

$$D_{total} = D_d \cdot \max(\delta_{xi}, \delta_{yi}) \cdot \gamma_x = 107.6\text{mm} \quad (1)$$

It should be noted that effective viscous damping coefficient ξ_{effb} , was defined to be equal to 15% of the critical damping, which is the lower limit of the effective viscous damping range, as stated by Kelly (2001).

Table 1 Eigenperiods and effective mass participation factors of the base-isolated building

Eigenmode	Eigenperiod (sec)	Effective modal masses participation factors		
		Ux (%)	Uy (%)	Rz (%)
1 st	1.292	99.8	≈ 0	28.9
2 nd	1.266	≈ 0	≈ 100	41.7
3 rd	1.114	≈ 0	≈ 0	29.3

Table 2 Mechanical characteristics of NRBs and LRBs

	NRB	LRB
Mass (kg)	111.60	117.30
Weight (kN)	1.0000	1.1507
Design displacement (mm)	94.90	94.90
Effective stiffness (kN/m)	722460	509730
Translational effective stiffness (kN/m)	664.8	1319.5
Elastic stiffness (kN/m)	664.8	20383.5
Rotational effective stiffness (kN.m/rad)	12.4330	12.4201
Yield strength (kN)	-	55.1985
Post yield stiffness ratio	-	0.031565

Subsequently, according to EC8 §3.2.2.2 (3), the elastic design spectrum is corrected by multiplying it with the coefficient $\eta = \sqrt{10/5 + \xi}$, where, ξ , is the viscous damping ratio, as a percentage. An approximate calculation of the displacement of the system at the isolation level, D_d , was then made by Eq. (2).

$$D_d = \frac{S_d(T_{d\text{tar}}, \xi_{\text{effb}})}{4\pi^2} \cdot T_{d\text{tar}}^2 = \frac{0.3125g \cdot \sqrt{10/5 + 15}}{4\pi^2} \cdot 1.2^2 = 0.07907 \quad (2)$$

Moreover, the torsional effects on a single seismic isolator are defined, by multiplying with a magnification coefficient, that was calculated by Eq. (3).

$$\delta_{xi} = 1 + \frac{e_{\text{tot},y}}{r_y} \cdot y_i \quad \text{and} \quad \delta_{yi} = 1 + \frac{e_{\text{tot},x}}{r_x} \cdot x_i \quad (3)$$

In which x_i and y_i are the relative displacements of the isolator i with respect to the center of the effective rigidity, in the X and Y directions, respectively.

The total 5% accidental mass eccentricities in the X and Y directions, respectively are defined by Eq. (4).

$$e_{\text{tot},x} = 0.05 \cdot L_x = 0.05 \cdot 24 = 1.2\text{m} \quad \text{and} \quad (4) \\ e_{\text{tot},y} = 0.05 \cdot L_y = 0.05 \cdot 20 = 1\text{m}$$

Lastly, the torsional radius r_x and r_y of the isolation system in the X and Y directions, respectively, which was equal in the two directions, due to the same stiffness of the isolators at the two structural horizontal axes, is defined according Eq. (5).

$$r_x^2 = \frac{\sum(x_i^2 \cdot K_{yi} + y_i^2 \cdot K_{xi})}{\sum K_{yi}} = 107.8019\text{m}^2 \quad \text{and} \\ r_y^2 = \frac{\sum(x_i^2 \cdot K_{yi} + y_i^2 \cdot K_{xi})}{\sum K_{xi}} = 107.8019\text{m}^2 \quad (5)$$

Therefore, the magnification coefficients for the X and Y directions equal $\delta_{xi} = 1.0928$ and $\delta_{yi} = 1.1336$, respectively.

Furthermore, according to the Annex 16 of the UBC 1997 Regulation, the calculation of the total design displacement, D_{total} , equals

$$K_{\text{eff},y} = \frac{W}{g} \cdot \left(\frac{2\pi}{T_{d\text{tar}}}\right)^2 = \frac{6252.051\text{kN}}{g} \cdot \left(\frac{2\pi}{1.2}\right)^2 \\ = 17.4723 \frac{\text{MN}}{\text{m}} \quad (6)$$

Therefore, the magnification coefficients for the X and Y directions equal $\delta_{xi} = 1.0928$ and $\delta_{yi} = 1.1336$, respectively.

Furthermore, according to the Annex 16 of the UBC 1997 Regulation, the calculation of the total design displacement, D_{total} , equals

$$D_{\text{total}} = D_d \cdot \left(1 + y \cdot \frac{12e}{b^2 + d^2}\right) = 93.1\text{mm} \quad (7)$$

In which b and d are the lengths of the elongated and the shorter side (24m and 20m), respectively, y is the half-length of the longitudinal dimension ($24/2 = 12\text{m}$) and e is the 5% of the length of the longitudinal dimension of the building ($e = 0.05 \cdot 24\text{m}$).

2.3 Selected earthquake records

Two sets of NF and FF accelerograms obtained from the Pacific Earthquake Engineering Research Center Database (beta version) are used for the analyses in this research study. The near- and far-fault seismic ground motions had been recorded during the same seismic events but at different stations. As already stated in previous studies (Somerville, 2005), in order to achieve more accuracy, two acceleration records are considered simultaneously in the two horizontal directions, the Fault-Normal (FN) and Fault-Parallel (FP) for each ground motion. The simulated building is subjected to 7 sets of NF and 7 sets of FF earthquakes, with simultaneous application of each seismic component along the X and Y directions of the building. It should be noted that 7 pairs of seismic ground motions have been selected according to the provisions of EC8, but, in order to generalize the results of this research work, a larger number of seismic ground motions should be used.

The selection of the NF ground motions is based on specific criteria: (i) an earthquake magnitude of $M_w \geq 6.0$ and (ii) a distance to the fault rupture of $R_{rup} < 20 \text{ km}$. The FF accelerograms are selected from the same seismic event, but had been recorded at a further distance from the fault $R_{rup} > 40 \text{ km}$. Relevant information for the selected near- and far-fault excitations is provided in Tables 3 and 4, respectively. In order to have compatible response results, both NF and FF ground motion records are normalized to have their peak ground accelerations (PGA) equal to $0.3g$. This value is selected, according to the requirements of EC8, which is the design ground acceleration, $a_g = 0.25g$, multiplied by the soil factor, $S=1.2$.

Subsequently, the spectral (or pseudo) acceleration response spectra of the near- and far-fault ground motions are constructed using the Seismo-Match Software, while considering a viscous damping ratio, $\xi=5\%$, and presented in Fig. 2 and 3 for the fault normal (FN) and fault parallel (FP) horizontal components, respectively. The black line provides the design target spectrum of the spectral accelerations, while the red line provides the mean value of the spectral accelerations for all selected seismic excitations. The scaling has been conducted using the elastic spectrum.

2.4 Seismic combinations and code provisions

It is known that the seismic response of buildings strongly depends on the direction of the imposed seismic excitations. Although the ideal design of an earthquake resisting building would require application of earthquake excitations in any direction, it is practically not possible to be applied for the design of all buildings, due to the enormous computational cost. Therefore, such detailed design analyses could only be performed for specific, high

Table 3 Description of selected horizontal NF records

EQ No.	NGA seq. no.	Event	Year	Station	M_w	F_N	F_P	R_{jb} (km)	R_{rup} (km)	V_{s30} (m/sec)
						PGA (g)	PGA (g)			
1	292	Irpinia- Italy-01	1980	Sturno	6.9	0.23	0.31	6.80	10.80	1000.0
2	802	Loma Prieta	1989	Saratoga Aloha Ave	6.93	0.36	0.38	7.60	8.50	370.80
3	1045	Northridge-01	1994	Newhall W Pico Canyon Rd.	6.69	0.43	0.28	2.1	5.5	285.9
4	1176	Kocaeli- Turkey	1999	Yarimca	7.51	0.28	0.31	1.40	4.80	297.00
5	1489	Chi-Chi- Taiwan	1999	TCU049	7.62	0.28	0.25	3.80	3.80	487.30
6	3746	Cape Mendocino	1999	Centerville Beach_ Naval Fac	7.01	0.32	0.48	16.44	18.31	459.04
7	764	Loma Prieta	1989	Gilroy Historic Bldg	6.93	0.29	0.24	10.27	10.97	308.55

Table 4 Description of selected horizontal FF records

EQ No.	NGA seq. no.	Event	Year	Station	M_w	F_N	F_P	R_{jb} (km)	R_{rup} (km)	V_{s30} (m/sec)
						PGA (g)	PGA (g)			
1	283	Irpinia Italy-01	1980	Arienzo	6.9	0.03	0.05	52.93	52.94	612.78
2	799	Loma Prieta	1989	SF Intern. Airport	6.93	0.24	0.33	58.52	58.65	190.14
3	946	Northridge-01	1994	Antelope Buttes	6.69	0.05	0.07	46.65	46.91	572.57
4	1154	Kocaeli Turkey	1999	Cekmece	7.51	0.05	0.05	64.95	66.69	346.0
5	2479	Chi-Chi Taiwan-04	1999	CHY057	6.2	0.08	0.08	78.16	78.45	411.46
6	826	Cape Mendocino	1992	Eureka - Myrtle and West	7.01	0.15	0.18	40.23	41.97	337.46
7	751	Loma Prieta	1989	Calaveras Reservoir	6.93	0.08	0.05	78.32	78.41	512.27

M_w : magnitude, R_{jb} : Restrict range of Joyner-Boore distance, R_{rup} : Restrict range of closest distance to rupture plane, V_{s30} : Average shear wave velocity of top 30 meters of the site.

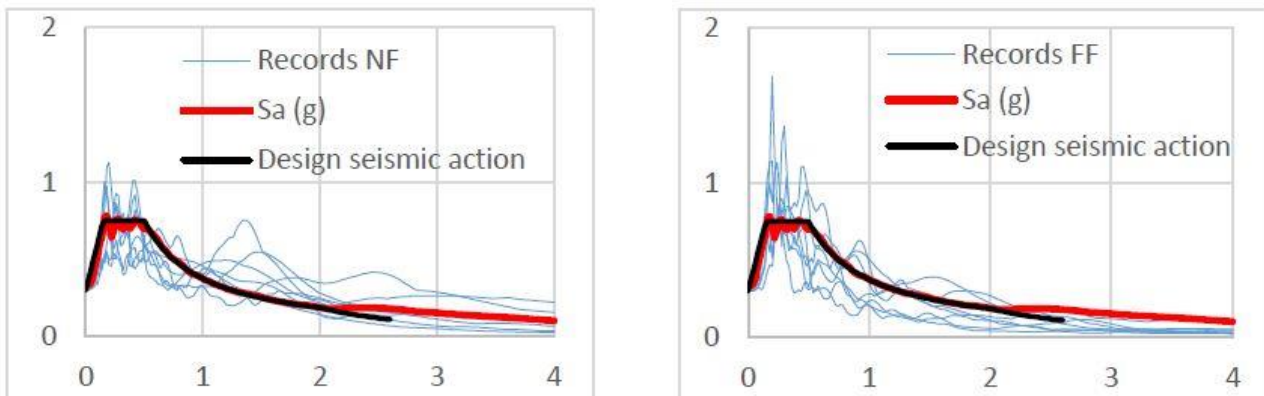


Fig. 2 Spectral acceleration response spectra and average response spectra for the selected (a) NF and (b) FF ground motions, fault normal (FN) direction

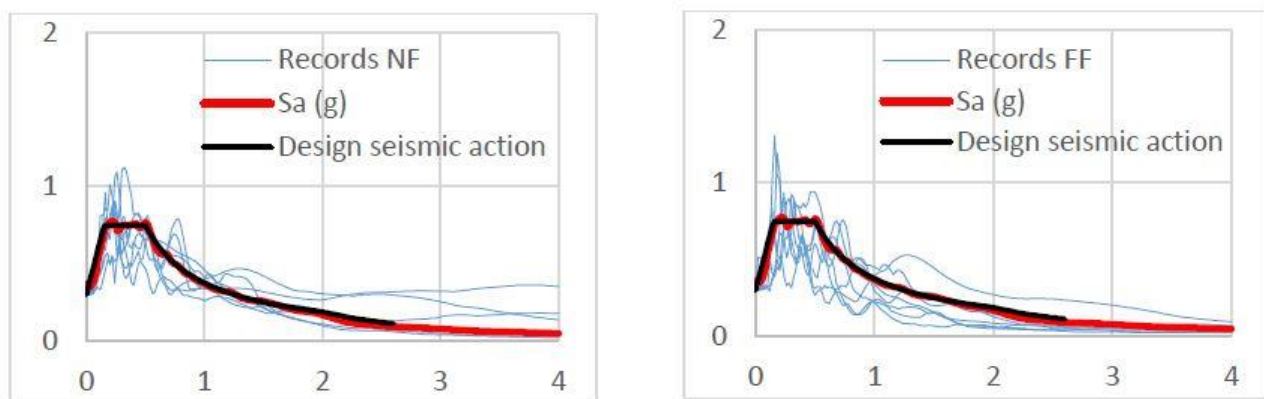


Fig. 3 Spectral acceleration response spectra and average response spectra for the selected (a) NF and (b) far-fault ground motions, fault parallel (FP) direction

importance buildings and thus, regulations have developed some simple combination rules in order to take into account the arbitrary direction of the seismic incident in the analysis.

For the purposes of this study, the provisions of EC8 (CEN, 2004b) are implemented. Specifically, a simultaneous action of the two orthogonal earthquake horizontal components is considered, by taking into account two independent loading cases and using the 100%+30% combination rule. Obviously, these combinations, with the reduction factors of 0.3, have been employed over the entire durations of the imposed excitations during the conducted time-history analyses.

Since the building is symmetrical with respect to the horizontal orthogonal axes passing through the geometric center of its plan, examining only the combinations below (with only a positive sign) is considered sufficient. Moreover, the 100% combination rule in both horizontal directions is also examined.

Thus, the building is examined under the following loading combinations:

- $G+0.3Q+E_x+E_y$
- $G+0.3Q+E_x+0.3E_y$
- $G+0.3Q+0.3E_x+E_y$

3. Analysis results

The time-history response of the simulated building is computed for each pair of seismic ground motions in order to investigate the influence of the excitation angle as well as the effect of imposing NF vs. FF seismic excitations on its peak seismic response in terms of the maximum relative displacements at the isolation level, interstory drifts and peak floor accelerations. Since the corner columns have the most extreme demands, the peak response results are extracted specifically for those columns and isolators in order to simplify the conducted parametric studies. The exact positions of all parameters investigated for their peak values, are shown in Fig. 4.

3.1 Maximum relative displacements at the isolation level

The estimation of the maximum relative displacements at the isolation level is very crucial as they are used to assess the minimum required width of the seismic gap that should be provided as a clearance around the base-isolated building in order to prevent structural pounding with the surrounding moat wall or/and adjacent structures. Specifically, when applying the loading combination $G+0.3Q+E_x+E_y$ to the building (Fig. 5), it is shown that the seismic gap should be above 154 mm in order to avoid collision in both X and Y directions.

A comparison of the computed maximum relative displacements at the isolation level with the required width of the seismic gap as determined from the relationships of commonly used seismic design codes reveals that the provisions of the latter might be insufficient. Specifically, the minimum required seismic gap according to the provisions of EC8 and UBC 1997 should be 107.6 mm and

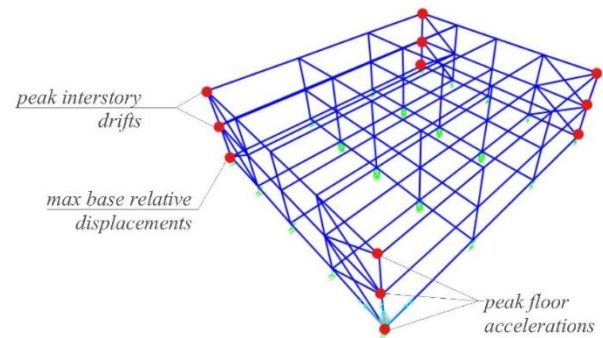


Fig. 4 Exact positions of peak interstory drifts, maximum base relative displacements and peak floor accelerations, taken for the four corner columns (shown in red bullets)

93.1 mm, respectively, for PGA equal to 0.3 g. Thus, both regulations underestimate the required seismic gap in this case by 30% and 39.5%, respectively.

Regarding the effect of the NF vs. FF ground motions, it is revealed that in most cases under consideration, the NF excitations can cause higher structural response of the base isolated building, in both X and Y directions. However, it should also be noted that, in some cases, under specific excitation angles, higher maximum relative displacements at the isolation level might occur under the FF ground motions. How much is the difference between the maximum relative displacements at the isolation level due to the NF and the FF ground motions, strongly depends on the excitation angle, which significantly affects the peak values of the maximum relative displacements at the isolation level and, thus, the width of the seismic gap that should be provided.

Similarly, Fig. 6 provides the corresponding maximum relative displacements at the isolation level for the loading combination $G+0.3Q+E_x+0.3E_y$, for which the width of the provided seismic gap of the base-isolated building should be at least 160 mm. When comparing this value with the previously computed values according to the provisions of the two aforementioned design codes, it is concluded that both regulations underestimate the required width of the seismic gap, in this case, by 33% and 42%, respectively. It is also observed that, although under two seismic events (Italy and Chi-Chi excitations) the structural response due to both the NF and FF ground motions is almost the same, for the rest of the seismic excitations, significantly larger maximum relative displacements at the isolation level are caused by the NF ground motions.

Next, the corresponding results for the loading combination $G+0.3Q+0.3E_x+E_y$ are displayed in Fig. 7, according to which the minimum required seismic gap is 135mm under both NF and FF ground motion. These results are compared with the values calculated according to the provisions of the two aforementioned design codes, showing that both regulations underestimate the actually required width of the provided seismic gap, in this case, by 20% and 31%, respectively.

It is observed that under some specific seismic events the peak response of the building in terms of the maximum relative displacements at the isolation level is almost at the

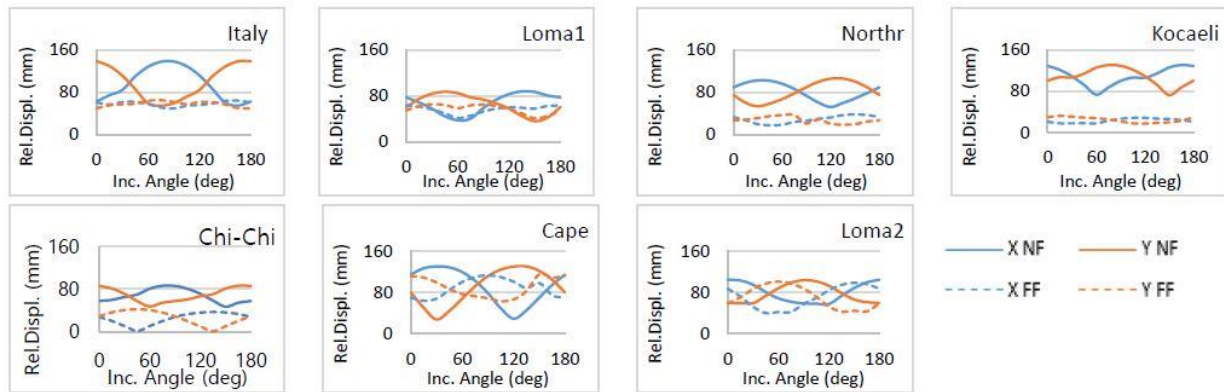


Fig. 5 Maximum relative displacements at the isolation level in X and Y directions of the base-isolated building in terms of the excitation angle, under the NF and FF ground motions, for the loading combination $G+0.3Q+Ex+Ey$

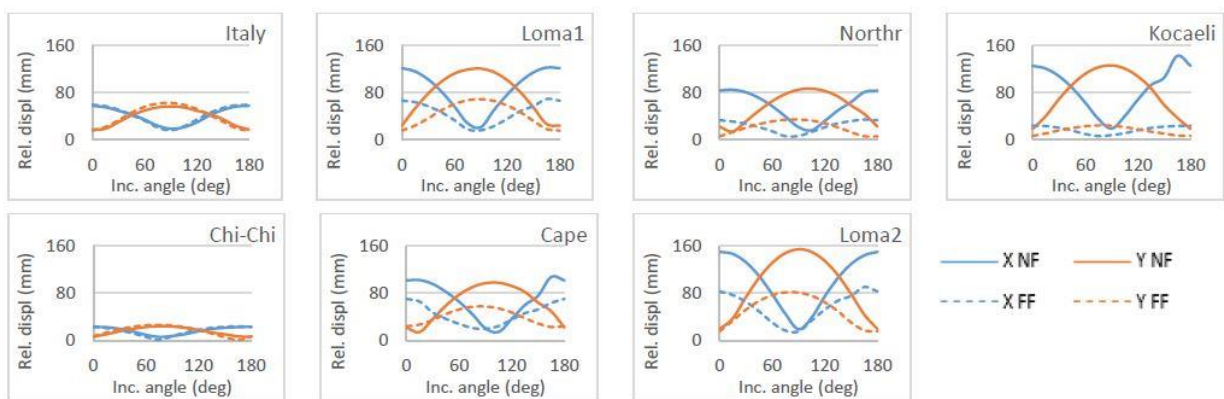


Fig. 6 Maximum relative displacements at the isolation level in the X and Y directions of the base-isolated building in terms of the excitation angle, under NF and FF ground motions, for the loading combination $G+0.3Q+Ex+0.3E$

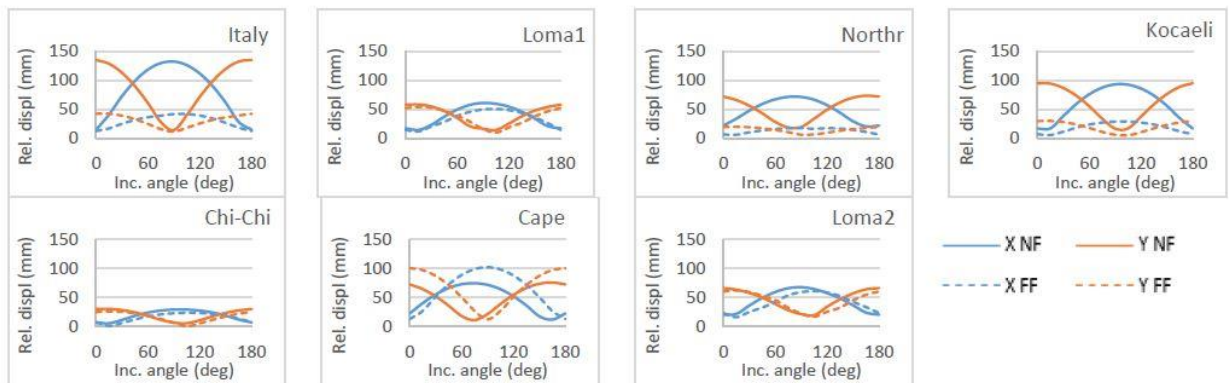


Fig. 7 Maximum relative displacements at the isolation level in the X and Y directions of the base-isolated building in terms of the excitation angle, under NF and FF ground motions, for the loading combination $G+0.3Q+0.3Ex+Ey$

same levels due to both NF and FF ground motions. However, under the rest of the seismic events, larger maximum relative displacements at the isolation level are caused due to the NF ground motions. As mentioned by Bray *et al.* (2004), the NF ground motions cannot be all assumed as the “worst case scenarios” for the design of all buildings. This trend strongly depends on the type of the directivity effect, for example on forward-directivity ground motions, most of the energy is concentrated on the narrow-

period and centered on the pulse period. Therefore, lower magnitude effects might produce more damaging ground motions for stiff buildings. Hence, it can be concluded that, when imposing NF ground motions to a base isolated building, it is likely for the building to exhibit higher peak seismic response, even though this observation does not apply in all cases.

Subsequently, in order to examine whether the combination $G+0.3Q+Ex+Ey$, with both components of the

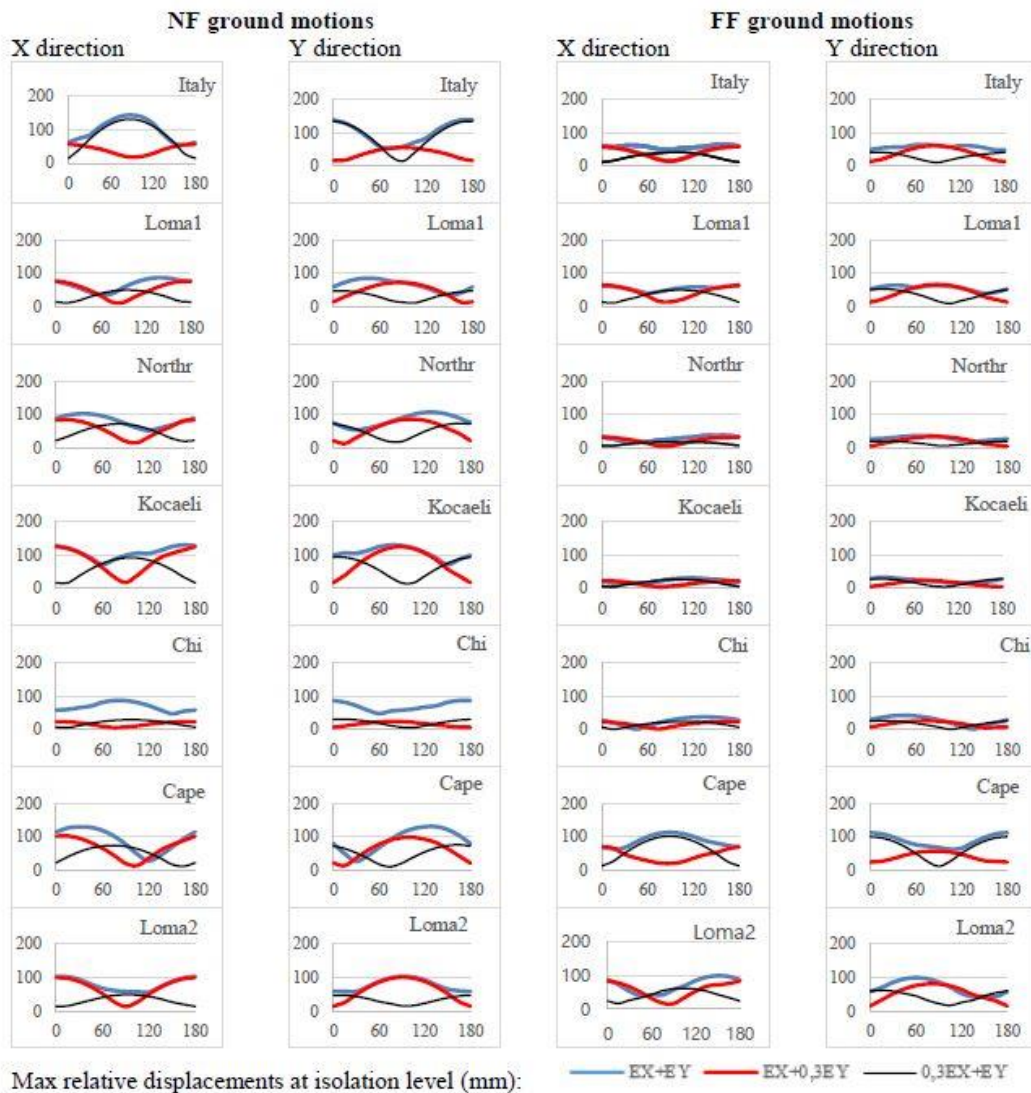


Fig. 8 Maximum relative displacements at the isolation level (mm) in the X and Y directions, in terms of the excitation angle (0-180o), under the NF and the FF ground motions for the three examined loading combinations: $G+0.3Q+E_x+E_y$, $G+0.3Q+E_x+0.3E_y$ and $G+0.3Q+0.3E_x+E_y$

earthquake excitation remaining unreduced, causes higher peak seismic response of the base-isolated building than the combinations with the component in the one direction reduced, an overall comparison between these three different loading combinations is presented in Fig.8. Specifically, the peak relative displacements at the base isolation level, as resulted from the analyses under NF and FF ground motions, in both X and Y directions are compared for the three loading combinations.

The computed maximum relative displacements at the isolation level indicate that, in both X and Y directions, under some specific seismic ground motions the maximum relative displacements at the isolation level occur for the loading combination $G+0.3Q+E_x+E_y$. Therefore, when performing dynamic analyses for the design of a base-isolated building according to the provisions of EC8, the maximum relative displacements at the isolation level may be underestimated, and consequently, the minimum

requirements for the width of the perimeter seismic gap may be underestimated. This observation applies under both NF and FF ground motions.

It should be further noted that, when comparing the maximum relative displacements at the isolation level due to the NF and the FF ground motions, a greater difference between the aforementioned loading combinations occurs under the NF ground motions and the significance of the incident angle is much greater and should not be ignored in case of NF excitations.

3.2 Peak interstory drifts

Correspondingly, an overall comparison between the three loading combinations (without and with 70% reduction of the seismic component in the one direction) in terms of interstory drifts is presented in Fig. 9. In particular, the envelopes of the peak interstory drifts at the corner

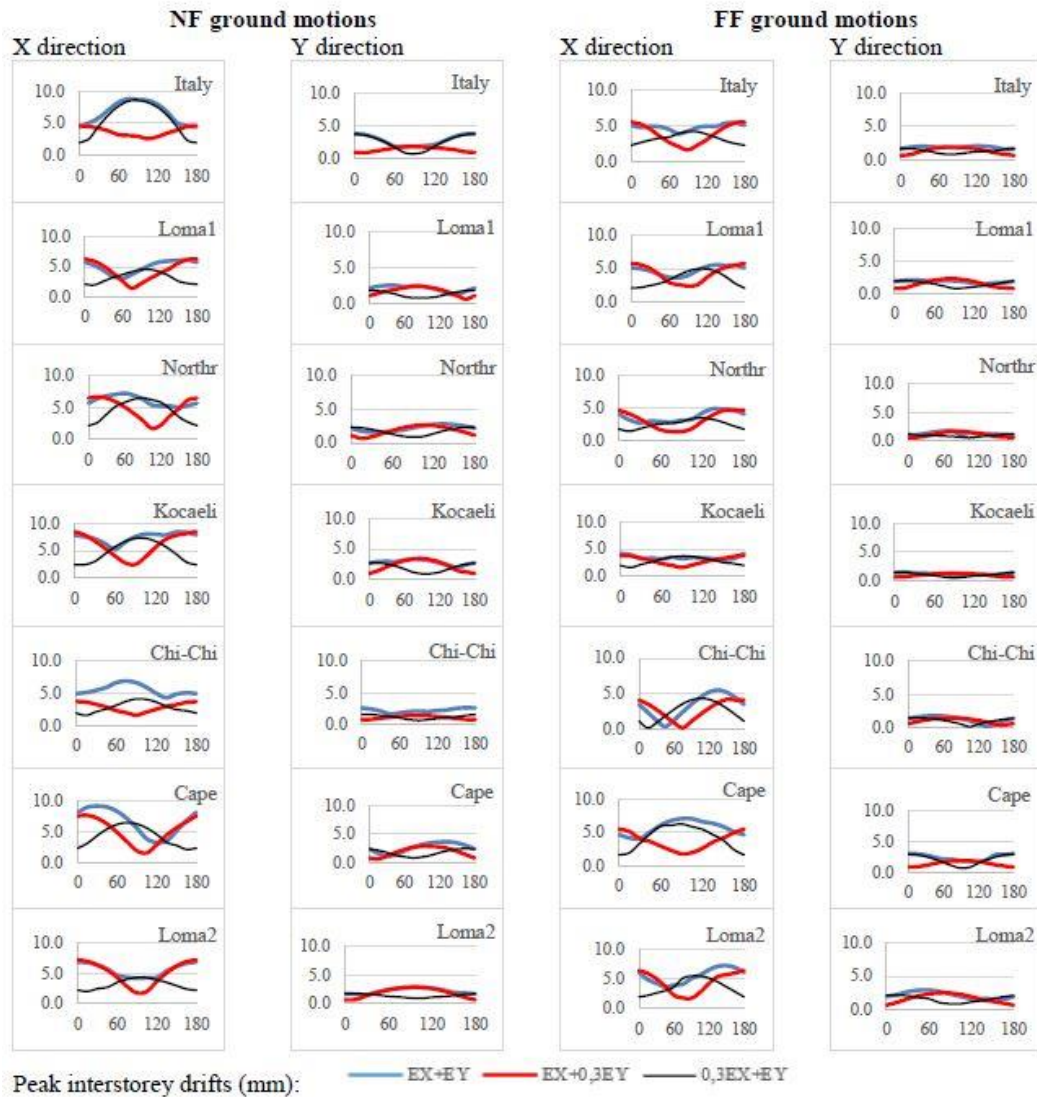


Fig. 9 Peak interstorey drifts in the X and Y directions, in terms of the excitation angle (0-180°), under both NF and FF ground motions for the three examined loading combinations

columns are provided, for various incident angles of the imposed seismic excitations.

The computed results indicate that, for the combination $G+0.3Q+E_x+E_y$, greater values occur when NF ground motions are imposed to the seismically isolated building under most seismic events but, at the same time, it appears that the peak interstorey drifts depend on both the excitation's frequency content and the incident angle. Specifically, it is shown that, the critical angles for each ground motion significantly differ in X and Y directions. Hence, no generalization regarding the critical incident angle can be made. The only relation between the peak interstorey drifts in X and Y directions is their phase difference of 90° between the critical incident angles, which is always observed in the specific symmetric building under investigation. It is thus, important to examine the seismic response of a building by imposing pairs of seismic ground motions along several excitation angles at the design stage, and not only along the building's major horizontal construction axes.

The peak seismic response of the base-isolated building for the other two seismic loading combinations ($G+0.3Q+E_x+0.3E_y$ and $G+0.3Q+0.3E_x+E_y$), exhibits an important uniformity regarding the critical incident angle. Specifically, the maximum of the peak interstorey drifts occurs in either 0° or 90° , in both X and Y directions, as already stated by Kostinakis *et al.* (2017). Finally, it should also be noted that the critical incident angles in X and Y directions are complementary angles, meaning that they always add up to 90° , in the specific symmetric building under investigation. Furthermore, the angle that gives the greater seismic response in the X direction, gives the smallest response in the Y direction, and vice versa.

Regarding time-history analysis, EC8 mentions the following: “The action effects due to the combination of the horizontal components of the seismic action may be computed using both of the two following combinations: a) $E_x+0.3E_y$ and b) $0.3E_x+E_y$ (4.3.3.5.1 (3), EN 1998-5)”. The above results justify to some extent the specific provisions of the EC8, as the critical incident angle is indeed at the two

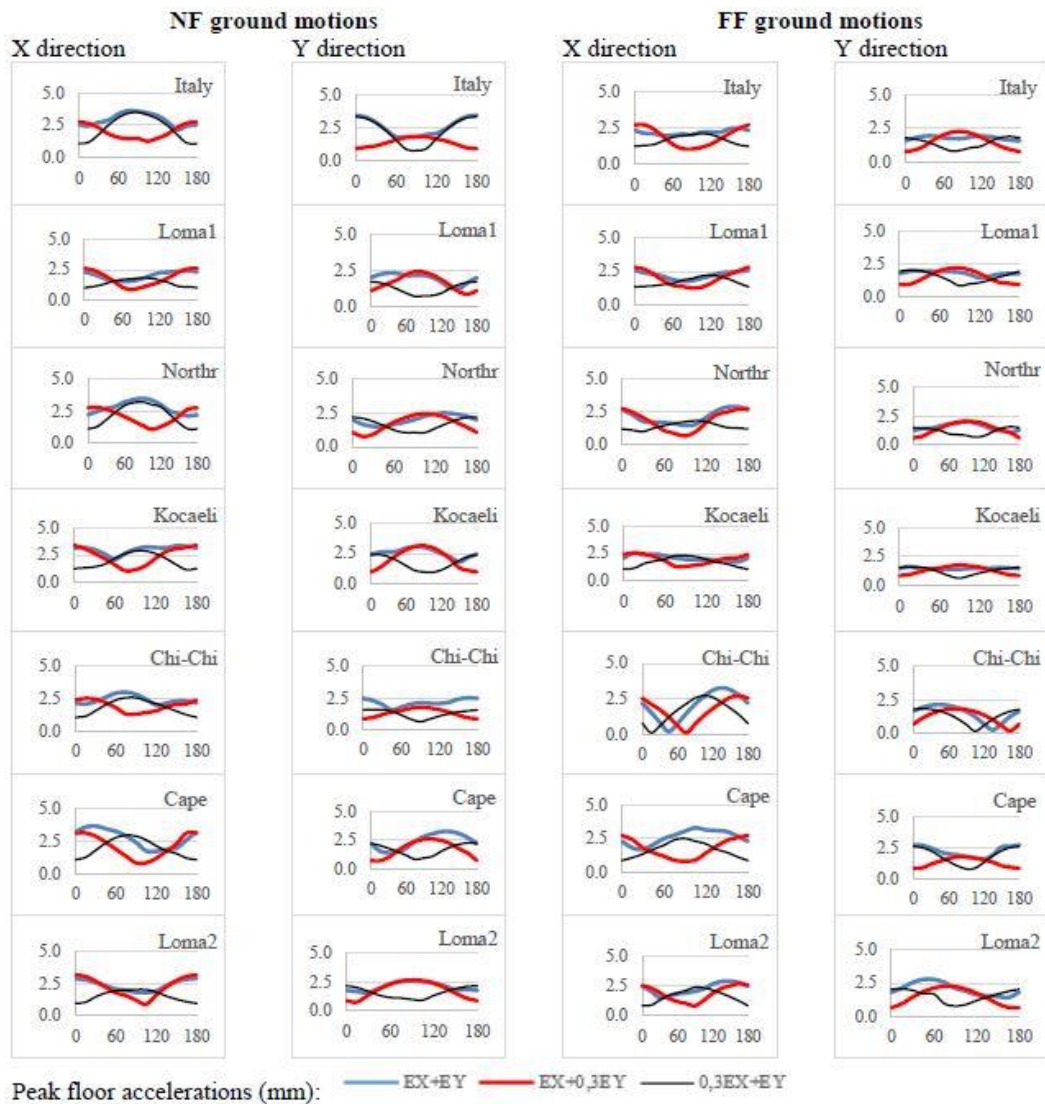


Fig. 10 Peak floor accelerations in X and Y directions in terms of the excitation angle (0-180°), under both NF and FF ground motions for the three examined loading combinations

orthogonal horizontal axes for most ground motions, under the two specific loading combinations with the seismic component in the one direction reduced by 70%.

While for some seismic records the peak interstory drifts under the NF pair are considerably greater than the corresponding drifts under the FF pair in both X and Y directions, for some other seismic records the difference between the NF and FF ground motions is insignificant, especially in the Y direction. Specifically, for the loading combination $G+0.3Q+E_x+0.3E_y$ in the X direction of the Italy seismic ground motion, the peak interstory drifts are at the same levels under both NF and FF pairs. Likewise, the same observation occurs in the Y direction for the Italy and the Loma Prieta-1 seismic events.

The extent of that difference strongly depends on the angle of incident. It is observed that when considering the two loading combinations, as specified in EC8, the peak interstory drifts are calculated adequately, but under some specific excitations (i.e., Cape Mendocino and Chi-Chi

seismic records) greater interstory drifts occur under the loading combination without any reduction in the one of the two directions.

Although under most cases the loading combination $G+0.3Q+0.3E_x+E_y$, which is applied to the building in accordance to the provisions of EC8 is sufficient, on the other hand, under some specific seismic records and for some specific excitation angles, the maximum of the peak interstory drifts occur under the loading combination $G+0.3Q+E_x+E_y$. This observation indicates that using solely the two seismic loading combinations suggested by the EC8, may underestimate the peak seismic response of a base-isolated building.

3.3 Peak floor accelerations

Finally, an overall comparison between the 3 loading combinations is presented in terms of the peak floor accelerations in Fig. 10, in X and Y directions, respectively,

under both NF and FF ground motions. By comparing the peak floor accelerations under the NF and FF excitations for these loading combinations, greater accelerations occur under the NF ground motions, for most seismic events, except the Chi-Chi (in X direction) and the Loma Prieta-2 (in Y direction) seismic events.

Moreover, for every seismic ground motion, there is a different critical incident angle and thus, no general rule regarding the critical angle can be extracted. In particular, different incident angles are observed between X and Y directions under each seismic event, but also between the NF and FF ground motions. The only relevance that can be seen is that, under each seismic ground motion, either a NF or a FF pair, the critical incident angles in X and Y directions are 90° out of phase in the specific symmetric building under investigation.

On the other hand, for the other two seismic loading combinations $G+0.3Q+Ex+0.3Ey$ and $G+0.3Q+0.3Ex+Ey$, an important uniformity is again observed regarding the critical incident angle. Specifically, the maximum of the peak interstory drifts occurs in either 0° or 90°, in both X and Y directions in the case of symmetric structures. This is an important observation, as it basically confirms the provisions of EC8, which suggests performing analyses for the loading combinations $G+0.3Q+Ex+0.3Ey$ and $G+0.3Q+0.3Ex+Ey$ and applying the ground accelerations along the two major horizontal construction axes simultaneously, without any other provisions for considering different excitation angles. It should be noted that these observations cannot be generalized, as they are valid only for symmetric structures.

4. Effect of accidental mass eccentricities

Many modern buildings exhibit torsional effects when dynamically excited, due to inherent eccentricities. Due to the fact that usually distributions of the floor loads are non-uniform and masonries are not symmetrically located at each floor, it is possible that torsional effects due to mass eccentricities may occur even in absolutely symmetrically designed buildings. Essentially, torsional effects may be observed even in absolutely symmetrically designed buildings due to uncertainties in determining the centers of mass and rigidity, as well as possible influence of torsional ground motion input. In such cases, the columns of the buildings are subjected to loads arising from both horizontal translations and the rotation of the building around the vertical axis.

In the specific case of the symmetric steel building under consideration, mass eccentricities, e_s , are obtained by shifting the centers of mass (CMs) from the centers of stiffness (CRs) of the superstructure, which are located in the geometric centers of the plans of all floors of the symmetric structure investigated in this research work.

The EC8 and the International Building Code (IBC) specify 5% eccentricities of the maximum floor dimension in each horizontal direction, while the New Zealand and Canadian codes suggest a value of 10%. The above codes require the relocation of the mass center in each floor along

the X and Y construction axes, in both positive and negative directions (Anagnostopoulos *et al.*, 2015a).

Previous research works have shown that the accidental mass eccentricities may cause higher torsional amplification. Specifically, Tena-Colunga *et al.* (2007), performed nonlinear dynamic analyses in order to study the peak seismic responses for different ratios of the static eccentricities between the CMs and CRs in the superstructure due to asymmetries. They observed that a higher torsional amplification exists in base-isolated buildings with mass eccentricities in the superstructure than in base-isolated buildings with stiffness eccentricities in the superstructure. On the other hand, Tsourekas *et al.* (2013) studied the influence of the mass eccentricity on the structural response within the context of Response History Analysis under three translational ground motion components and concluded that the observed variation is not considerable and unsubstantial in some cases. According to Lee (1980), base isolation reduced the structural torques significantly, even if the building had large eccentricities. In the same research work, it was also stated that that reduction of the structural torques was greatest when the isolation system's center of stiffness coincided with the building's center of mass. Jangid *et al.* (1993) studied the nonlinear response of a torsionally coupled base isolated building to two-component random ground motion and revealed that the effectiveness of base isolation was reduced for higher eccentricities.

Polycarpou *et al.* (2015) showed that the degree by which the incident angle affects the amplifications of columns deflections was not significantly affected by the mass eccentricities. On contrary, they pointed out that it depended more on the characteristics of the seismic ground motions.

Anagnostopoulos *et al.* (2015b) summarized the modeling approaches of earthquake-induced torsion in buildings and pointed out that, although building codes allow simplified assumptions and idealizations of one-story models, those may lead to erroneous conclusions. Therefore, the simplified assumptions proposed by several building codes need to be further investigated.

Tena-Colunga *et al.* (2006) examined whether the 10% accidental mass eccentricity in the superstructure of a base isolated building is adequate. They concluded that the torsional plan eccentricity for the isolation system should not exceed 10% of the plan dimension in the given direction of analysis. In addition, they noted that a building has a strong torsional irregularity when the torsional plan eccentricities exceed 20% of the plan dimension in the given direction of analysis and when the torsional plan eccentricity for the isolation system exceeds 15% of the plan dimension in the given direction of analysis. Furthermore, by performing nonlinear time response analyses in symmetric and asymmetric in plan buildings, Kostinakis *et al.* (2015) showed that the structural eccentricity significantly affected the seismic damage level, causing most severe damages among the asymmetric systems.

Kilar *et al.* (2009) examined the nonlinear response of asymmetric base-isolated buildings with various positions

of the center of isolators (CI). The bearings were positioned in a way that the eccentricity of the isolation system matched the eccentricity of the superstructure. Thus, the CI always corresponded to the actual center of masses CM. It was concluded that when the CI coincided with the CM, the torsional amplifications in the base isolation system were significantly reduced. On the other hand, it was found that such a distribution does not protect well the superstructure, since the top flexible side displacement can be increased up to ~ 2 times with respect to a symmetric structure. This is mainly due to the fact that in that case the eccentricity of the superstructure between the center of stiffness and the CM remains, and keeps contributing to the torsion of the superstructure.

In order to examine the effect of accidental mass eccentricities, nonlinear dynamic analyses are performed, in order to assess the peak seismic responses for different bidirectional mass eccentricities, in both X and Y directions, at all levels of the superstructure, as shown in Fig. 11. Because the corner columns have the most extreme demands, the results are extracted for those columns and isolators, in order to simplify the procedure. The precise positions for the extracted results presented in the following subsections are exactly those that are shown in Fig. 4. In the symmetric base-isolated building, the same results are computed for all 4 corner columns, while for the two cases with accidental mass eccentricities the results differ in each element. For the sake of brevity, only analyses for the loading combination $G+0.3Q+Ex+Ey$ are performed in these parametric studies. The polar plots that are provided in Section 4 use polar axes, where the distance, in the radial direction, from the pole denotes the value of the parameter that is examined and the angle corresponds to the incident angle of the imposed seismic excitation.

4.1 Maximum relative displacements at the isolation level

Theoretically, when considering accidental mass eccentricities at the superstructure, the seismic response of the base-isolation system will be increased. In order to examine and verify this assumption, the envelopes of the peak relative displacements at the base isolation level extracted from the four corner columns are presented in this paragraph, for the symmetric base-isolated building versus the two buildings with bidirectional accidental mass eccentricities of 5% and 10%.

Specifically, an overall comparison of the three different types of buildings in terms of the peak relative displacements is illustrated by the polar plots that are provided in Figs. 12 and 13, under NF and FF ground motions, in X and Y directions respectively, among all excitation angles. In particular, the polar plots provide the maximum relative displacements at the base isolation level as the distance from the pole along the radial direction, where the two grey circles correspond to 100 mm and 200 mm, in terms of the incident angle of the imposed seismic excitation, which corresponds to the angle of the polar plots.

The computed results indicate that the peak relative

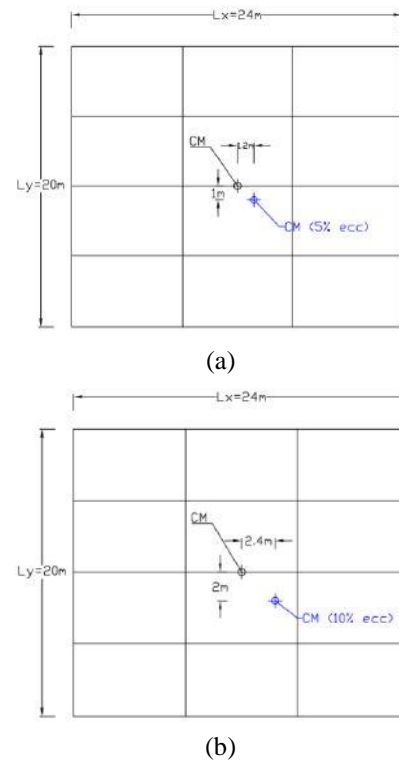


Fig. 11 Direction of (a) 5% and (b) 10% accidental mass eccentricities at each floor

displacements in both X and Y directions are significantly increased due to the accidental mass eccentricities and, as expected, the building with 10% accidental mass eccentricities presents greater relative displacements at the base isolation level.

Under almost all seismic events, the maximum relative displacements at the isolation level due to the NF ground motions are considerably larger than the corresponding values due to the FF ground motions, in both X and Y directions, and among all excitation angles. The only exception is the seismic event in Cape Mendocino, where the maximum relative displacements at the isolation level are equally large under both NF and FF ground motions. It should also be noted that, under each seismic ground motion a different critical incident angle occurs.

Regarding the incident angle, the behavior of the superstructure, in general, remains the same for all three different cases that are considered (specifically, without any eccentricities, with 5% eccentricities and with 10% eccentricities), with slightly increased structural response, when considering accidental mass eccentricities. Thus, accidental mass eccentricities should be considered for the seismic design of a base-isolated building, as they cause an increase of the required clearance around a seismically isolated building in order to avoid structural pounding and its detrimental consequences.

4.2 Peak interstory drifts

Subsequently, the peak interstory drifts of the

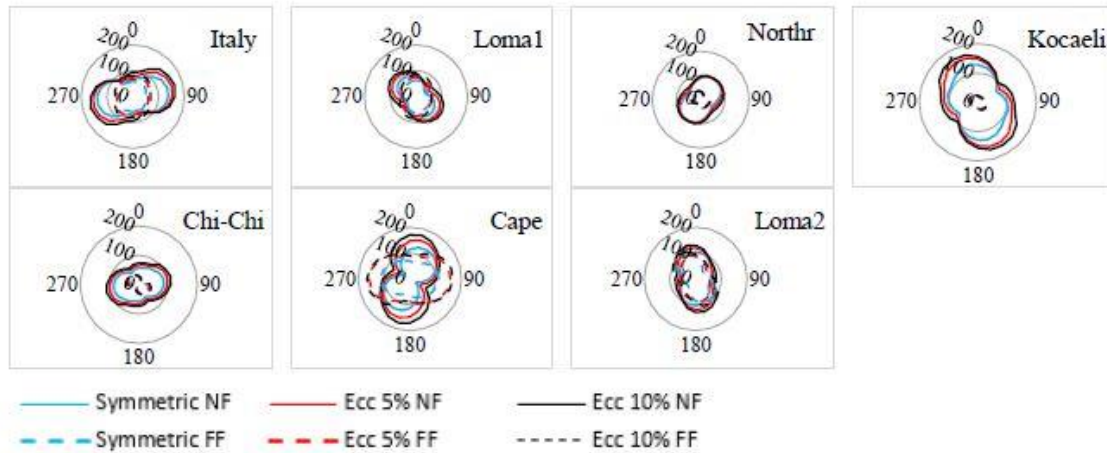


Fig. 12 Peak relative displacements (mm) at the isolation level in the X direction under NF and FF ground motions, in terms of the excitation angle while considering symmetric and non-symmetric (5% and 10%) base isolated buildings

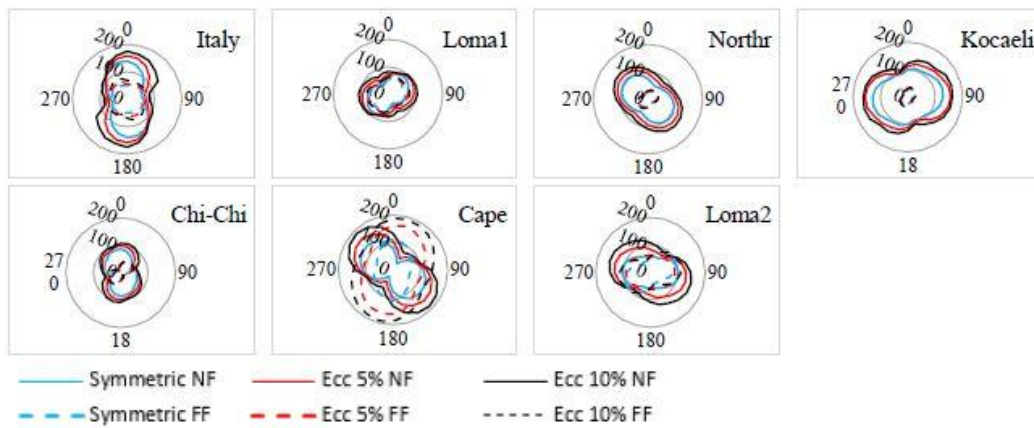


Fig. 13 Peak relative displacements (mm) at the isolation level in the Y direction under NF and FF ground motions, in terms of the excitation angle while considering symmetric and non-symmetric (5% and 10%) base isolated buildings

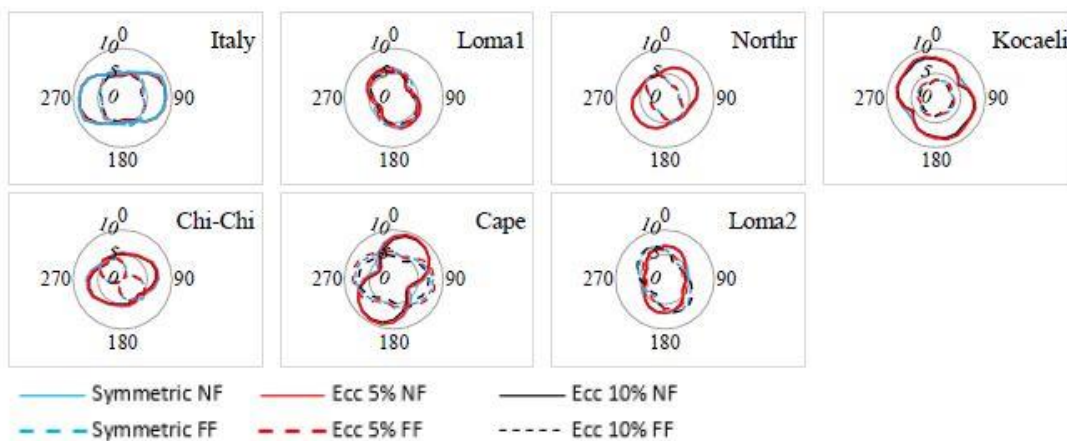


Fig. 14 Maximum interstory drifts (mm) in the X direction under NF and FF ground motions, in terms of the excitation angle, for symmetric and non-symmetric (5% and 10%) base isolated buildings

superstructure are examined, in order to investigate whether the accidental mass eccentricities influence this parameter. Specifically, the overall comparison between the peak interstory drifts computed at the symmetric base-isolated

building and the buildings with 5% and 10% accidental mass eccentricities is presented in the Figs. 14 and 15, for the X and Y directions, respectively. Specifically, the polar plots in Fig. 14 and Fig. 15 provide the peak interstory

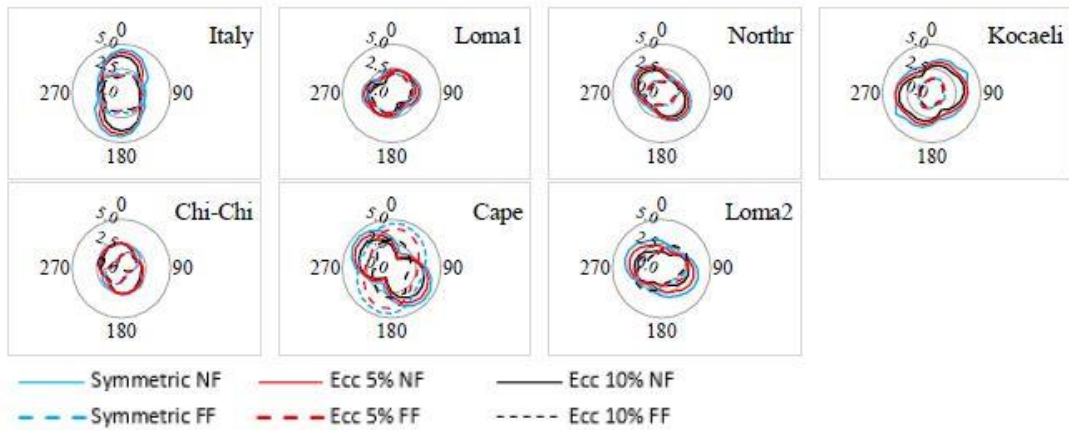


Fig. 15 Maximum interstory drifts (mm) in the Y direction under NF and FF ground motions, in terms of the excitation angle, for symmetric and non-symmetric (5% and 10%) base isolated buildings

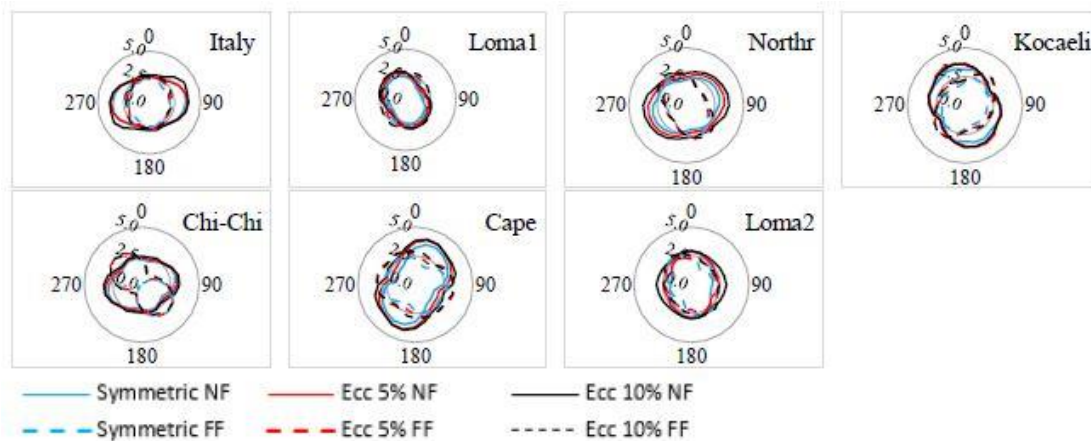


Fig. 16 Maximum floor accelerations (m/s^2) in the X direction under NF and FF ground motions, in terms of the excitation angle for symmetric and non-symmetric (5% and 10%) base isolated buildings

drifts as the distance from the pole along the radial direction, where the two grey circles correspond to 5 and 10 mm in Fig. 14 and 2.5 and 5 mm in Fig. 15, in terms of the angle of the polar plots, which represents the incident angle of the imposed seismic excitation.

According to the computed peak response, it is generally observed that, regarding the maximum of the peak interstory drifts, the seismic performance of the building is generally greater when subjected to NF ground motions, in both X and Y directions, but on the contrary, this increase is strongly related to the incident angle. In almost all cases, the occurred interstory drifts of the building with 10% accidental mass eccentricities due to NF ground motions are up to 50% increased. This is an important observation, since it is effective for most of the incident angles. On the other hand, it is worth noting that, for some specific excitation angles the peak interstory drifts due to the FF ground motions are greater than the corresponding values due to the NF ground motions.

When comparing the symmetric building and the buildings with 5% and 10% accidental mass eccentricities, minor differences of the peak interstory drifts are observed. Therefore, it can be concluded that, at least for the

interstory drifts, the accidental mass eccentricities do not influence significantly the peak response of the superstructure of the base-isolated building. Finally, it is again observed that the building presents different critical incident angle under each seismic event, which confirms the difficulty of specifying a priori the critical incident angle.

4.3 Peak floor accelerations

Similarly, a comparison between the peak floor accelerations of the base-isolated buildings with eccentricities (5% and 10%) and without any eccentricities is presented in X and Y directions, in Figs. 16 and 17, respectively. Accordingly, the polar plots in Fig. 16 and Fig. 17 provide the peak floor accelerations as the distance from the pole along the radial direction, where the two grey circles correspond to 2.5 and 5 m/s^2 in Fig. 16 and 2 and 4 m/s^2 in Fig. 17, in terms of the incident angle of the imposed seismic excitation.

In both X and Y directions, significant variations for the different excitation angles are observed, but at the same time, regarding the three different cases of the base-isolated

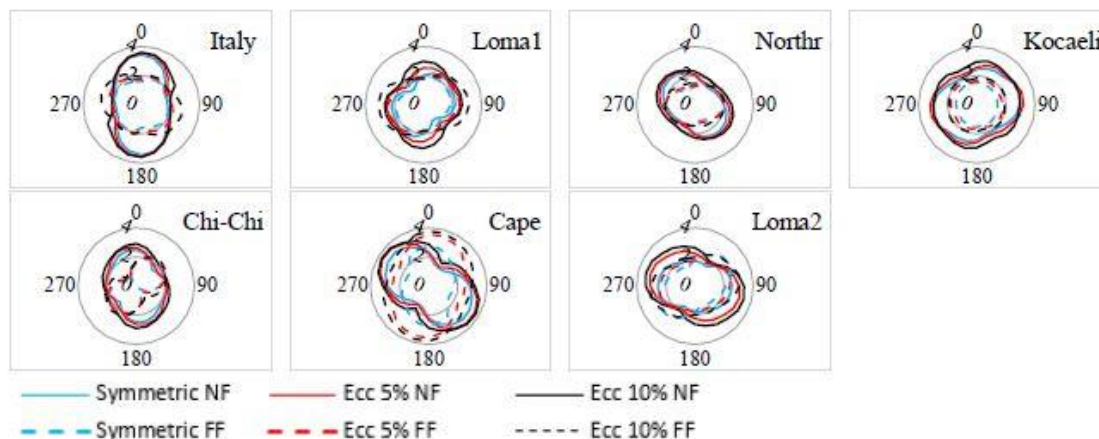


Fig. 17 Maximum floor accelerations (m/s^2) in the Y direction under NF and FF ground motions, in terms of the excitation angle for symmetric and non-symmetric (5% and 10%) base isolated buildings

building, a uniformity is observed. The results do not present important differences under most excitation angles, which leads to the conclusion that the accidental mass eccentricities do not significantly affect the peak seismic response of the base-isolated building, as already stated by Anagnostopoulos *et al.* (2015a), at least in terms of the peak floor accelerations of the superstructure. This observation applies under all ground motions, both NF and FF for the structure under consideration.

As expected, for most seismic records, the “worst case scenario” in terms of the peak floor accelerations, is the case of 10% bidirectional eccentricities of the base-isolated building. It is shown that the accidental mass eccentricities mainly increase the peak seismic response, but occasionally they may even decrease it. Which one happens and to what extent, strongly depends on the earthquake characteristics.

Regarding the two types of ground motions, although the peak values of the top-floor accelerations do not significantly differ, in most cases a slightly increased seismic response is observed under the NF ground motions. Moreover, the maximum floor accelerations clearly depend on the excitation angle, as under each pair of seismic records, the maximum floor acceleration occurs along a different incident angle, which leads to the conclusion that it is not possible to specify a priori the critical incident angle of a building without performing dynamic analyses with varying incident angles. Therefore, it can be concluded that the determining factor for the peak response of the seismic isolated system is the angle of incidence.

5. Concluding remarks

In the research work presented in this paper, the effect of NF and FF ground motions imposed on a base-isolated steel building has been investigated, considering various angles of seismic excitation, as well as the cases of mass eccentricities. The outcomes of the presented research work supplement and support conclusions of other relevant research studies, such as that the peak seismic response of the examined symmetric base-isolated steel building

indicates that the NF seismic pairs may cause more intense movement, than the corresponding FF seismic pairs. Thus, the effectiveness of seismic isolation seems to strongly depend on the proximity to active faults, as well as the incident angle of the imposed seismic excitation with respect to the principal horizontal construction axes.

Subsequently, from the investigation of the effect of the seismic incident angle, the results extracted in this work confirm that the critical angle of excitation is not always along the principal horizontal axes, 0 or 90 degrees, as already stated in preceding literature works (i.e. Kostinakis *et al.*, 2017). In particular, the maximum response occurs at different excitation angle for each pair of seismic records. It should be noted that this observation applies only for the loading combination $G+0.3Q+Ex+Ey$, acting on the examined symmetric base-isolated steel building. An interesting observation is that for the two loading combinations specified in the EC8 (i.e. $G+0.3Q+Ex+0.3Ey$ and $G+0.3Q+0.3Ex+Ey$), the peak seismic response present great uniformity in terms of the critical incident angle. Therefore, for these specific loading combinations, considering excitation angles other than the two orthogonal horizontal directions, might be unnecessary for a symmetric base-isolated building due to the dominance of the unreduced excitation component.

The overall conclusion regarding the effect of the critical incident angle is that, although in most examined cases the two combinations according to the provisions of the EC8 actually give the peak seismic response of the base isolated building, on contrary, under some specific seismic excitations and for specific incident angles, the loading combination $G+0.3Q+Ex+Ey$ without any reduction in any direction, causes greater peak seismic response to the structure. Thus, imposing the seismic excitations only along the principle horizontal construction axes for the seismic design of a symmetric base-isolated building, may lead to a significant underestimation of its actual peak seismic response. The determination of the critical incident angle is hence complicated or even impossible, and different simulations should be performed for each base-isolated building, in order to obtain a more reliable evaluation of the

peak seismic response.

A comparison of the minimum required dimension of the seismic gap as obtained from the analyses, with the corresponding dimensions as they arise from the relationships of two different design codes has also been made. It is shown that, both EC8 and UBC 1997 give a very close assessment of the seismic gap only under the loading combination $G+0.3Q+0.3E_x+E_y$. Under the other two examined loading combinations, the minimum required dimension of the seismic gap can be significantly underestimated for the specific case of a symmetric base-isolated building.

Moreover, by examining the effect of 5% and 10% bidirectional accidental mass eccentricities on the seismic response of the symmetric base-isolated building, it is confirmed that mass eccentricities generally increase the response of the symmetric base-isolated building, due to the increase of the torsional effects, which cause rotations of the diaphragms. However, rotation of the base-isolated building essentially is rotation of a rigid body. Specifically, the maximum relative displacements at the base isolation level are significantly increased due to the existence of mass eccentricities, either of 5% or of 10%. On contrary, regarding the deformations of the superstructure, minor differences are observed for both peak interstorey drifts and absolute floor accelerations due to the mass eccentricities, which leads to the conclusion that the superstructure of a symmetric base-isolated steel building practically may not be affected by the accidental mass eccentricities.

Furthermore, by comparing the results of near- and far-fault ground motions, no significant difference in the increase of the response is observed in the case of the symmetric base isolated building examined in this work. Additionally, this study indicates that when seismically designing base-isolated steel braced frame buildings, the influence of the accidental mass eccentricities both of $0.05L$ as per EC8, and of $0.1L$, might be relatively minor for the seismic response of the superstructure, except from the minimum required dimension of the seismic gap, which is significantly increased. Although mass eccentricities influence the maximum relative displacements at the isolation level, the deformation of the superstructure of the base isolated building under consideration is very insignificantly affected by potential mass eccentricities, as the isolated building moves essentially as a rigid body. This observation, which of course applies to the base-isolated steel building under consideration, suggests that considering accidental mass eccentricities in base-isolated buildings might be obsolete for the design of their superstructures, at least for torsionally stiff buildings. Nevertheless, consideration of mass eccentricities can be important for the estimation of the required seismic gap as they may lead to significant increase of the maximum relative displacements at the isolation level and potential structural pounding incidences.

In conclusion, it is confirmed that the peak seismic response of the base-isolated symmetric steel building strongly depends on the angle of the seismic incidence, which can also amplify or alleviate the effects of NF ground motions and mass eccentricities. The response induced at

excitation angles other than the construction horizontal directions (0° and 90°), which are usually the only directions used in the analysis according to most design seismic codes, could be highly increased. It should be noted that this remark is based on the study of a symmetric steel building and cannot be generalized. This observation should be considered for the seismic building design, contrary to some seismic codes, where no such provisions are included. Thus, it might be necessary to perform numerous dynamic analyses and impose the seismic loads under different incident angles, in order to determine the critical incident angle for the building under investigation. This is not a practical solution for the design of all earthquake resistant buildings, but for certain high importance projects, this may be inevitable. Of course, these observations are valid only for the base isolated steel building examined in this paper and further investigation is considered necessary in order to generalize them.

References

- Anagnostopoulos, S.A., Kyrkos, M.T. and Stathopoulos, K.G. (2015a), "Earthquake induced torsion in buildings: critical review and state of the art", *Earthq. Struct.*, **8**(2), 305-377. <http://dx.doi.org/10.12989/eas.2015.8.2.305>.
- Anagnostopoulos, S., Kyrkos, M., and Stathopoulos, K. (2015b), "Earthquake induced torsion in buildings: critical review and state of the art", *Earthq. Struct.*, **8**(2), 305-377. <http://dx.doi.org/10.12989/eas.2015.8.2.305>.
- Athanatopoulou, A.M. (2005), "Critical orientation of three correlated seismic components", *Eng. Struct.*, **27**(2), 3013-312. <https://doi.org/10.1016/j.engstruct.2004.10.011>.
- Bray, J. and Rodriguez-Marek, A. (2004), "Characterization of forward-directivity ground motions in the near-fault region", *Soil Dyn. Earthq. Eng.*, **24**, 815-828. <https://doi.org/10.1016/j.soildyn.2004.05.001>.
- CYS National Annex to CYS EN 1998-1:2004. Eurocode8: Design of buildings for earthquake resistance - Part 1: General rules, seismic actions and rules for buildings, *Nicosia, Eurocodes Committee, Scientific and Technical Chamber of Cyprus under a Ministry of Interior's Programme*.
- EN 1998-1:2004. Eurocode8: Design of buildings for earthquake resistance - Part 1: General rules, seismic actions and rules for buildings, *Brussels: European Committee for Standardization*.
- EN 1998-3:2005. Eurocode8: Design of buildings for earthquake resistance - Part 3: Assessment and retrofitting of buildings, *Brussels: European Committee for Standardization*.
- Fontara, I., Kostinakis, K., Manoukas, E. and Athanatopoulou, A. (2015), "Parameters affecting the seismic response of buildings under bi-directional excitation", *Struct. Eng. Mech.* **53**(5), 957-979.
- ICC. (2003). International Building Code, *International Code Council, Building Officials and Code Administration International Inc., Country Club Hills, IL., International Conference of Building Officials, Whittier, CA, Southern Building Code Congress International, Inc., Birmingham, Alabama*.
- Jangid, R. and Datta, T. (1993), "Seismic response of torsionally coupled structure with elastoplastic base isolation", *Eng. Struct.*, **16**, 256-262. [https://doi.org/10.1016/0141-0296\(94\)90065-5](https://doi.org/10.1016/0141-0296(94)90065-5).
- Kalkan, E. and Reyes, J. (2015), "Significance of rotating ground motions on behavior of systemetric and asymmetric-plan structures: part 2. case studies", *Earthq. Spectra*, **31**(3), 1613-1628. <https://doi.org/10.1193%2F072012EQS241M>.

- Kalkan, E. and Kwong, N. (2014), "Pros and cons of rotating ground motion records to fault-normal/parallel directions for response history analysis of buildings", *J. Struct. Eng.*, **140**(3). [https://doi.org/10.1061/\(ASCE\)ST.1943-541X.0000845](https://doi.org/10.1061/(ASCE)ST.1943-541X.0000845).
- Kilar, V. and Koren, D. (2009), "Seismic behaviour of asymmetric base isolated structures with various distributions of isolators", *Eng. Struct.*, **31**(4), 910-921. <https://doi.org/10.1016/j.engstruct.2008.12.006>.
- Kostinakis, K., Manoukas, G. and Athanatopoulou, A. (2017), "Influence of Seismic Incident Angle on Response of Symmetric in Plan Buildings", *KSCE J. Civil Eng.*, 1-11. <https://doi.org/10.1007/s12205-017-1279-1>.
- Kostinakis, K., Morfidis, K. and Xenidis, H. (2015), "Damage response of multistorey r/c buildings with different structural systems subjected to seismic motion of arbitrary orientation", *Earthq. Eng. Struct. Dyn.*, **44**(12), 1919-1937. <https://doi.org/10.1002/eqe.2561>.
- Kostinakis, K., Athanatopoulou, A. and Morfidis, K. (2015), "Correlation between ground motion intensity measures and seismic damage of 3D R/C buildings", *Eng. Struct.*, **82**, 151-167. <https://doi.org/10.1016/j.engstruct.2014.10.035>.
- Kostinakis, K., Athanatopoulou, A. and Avramidis I. (2012), "Orientation effects of horizontal seismic components on longitudinal reinforcement in R/C Frame elements.", *Nat. Haz. Earth Syst. Sci.*, **12**, 1-10. <http://www.nat-hazards-earth-syst-sci.net/12/1/2012/>.
- Kramer, S.L. (1996), *Geotechnical Earthquake Engineering*, Prentice-Hall, NJ, USA.
- Lagaros, N. (2010), "Multicomponent incremental dynamic analysis considering variable incident angle", *Build. Infrastruct. Eng.*, **6**(1-2), 77-94. <https://doi.org/10.1080/15732470802663805>.
- Lee, M. (1980), "Base isolation for torsion reduction in asymmetric structures under earthquake loading", *Earthq. Eng. Struct. Dyn.*, **8**, 349-359. <https://doi.org/10.1002/eqe.4290080405>.
- Magliulo, G., Maddaloni, G. and Petrone, C. (2014), "Influence of earthquake direction on the seismic response of irregular plan RC frame buildings", *Earthq. Eng. Eng. Vib.*, **13**(2), 243-256. <https://doi.org/10.1007/s11803-014-0227-z>.
- Mavroeidis, G., Dong, G. and Papageorgiou, A. (2004), "Near-fault ground motions, and the response of elastic and inelastic single-degree-of-freedom (SDOF) systems", *Earthq. Eng. Struct. Dyn.*, **33**(9), 1023-1049. <https://doi.org/10.1002/eqe.391>.
- NBCC. (1995). *National Building Code of Canada*, Institute for Research in Construction, National Research Council of Canada, Ottawa, Ont.
- New Zealand Government (1992), *The Building Regulations 1992*, Wellington.
- Nguyen, V.T and Kim, D. (2013), "Influence of incident angles of earthquakes on inelastic responses of asymmetric-plan structures", *Struct. Eng. Mech.*, **45**(3), 373-389. <https://doi.org/10.12989/sem.2013.45.3.373>.
- PEER Pacific Earthquake Engineering Research Center. Ground motion database (2011), http://peer.berkeley.edu/peer_ground_motion_database.
- Polycarpou, P.C., Papaloizou, L., Komodromos, P. and Charmpis, D.C. (2015), "Effect of the seismic excitation angle on the dynamic response of adjacent buildings during pounding", *Earthq. Struct.*, **8**(5), 1127-1146. <http://dx.doi.org/10.12989/eas.2015.8.5.1127>.
- Reyes, J. and Kalkan, E. (2015), "Significance of rotating ground motions on behavior of symmetric- and asymmetric-plan structures: part 1. parametric study", *Earthq. Spectra*, **31**(3), 1591-1612. <https://doi.org/10.1193%2F072012EQS241M>.
- Rigato, A. and Medina, R. (2007), "Influence of angle of incidence on seismic demands for inelastic single-storey structures subjected to bi-directional ground motions", *Eng. Struct.*, **29**(10), 2593-2601. <https://doi.org/10.1016/j.engstruct.2007.01.008>.
- Somerville, P. (2005), "Engineering characterization of near fault ground motions", *Proceedings of the 2005 NZSEE Conference*, Wairakei, NZ.
- Tena-Colunga, A. and Escamilla-Cruz, J.L. (2007), "Torsional amplifications in asymmetric base-isolated structures", *Eng. Struct.*, **29**(2), 237-247. <https://doi.org/10.1016/j.engstruct.2006.03.036>.
- Tena-Colunga, A. and Zambrana-Rojas, C. (2006), "Dynamic torsional amplifications of base-isolated structures with an eccentric isolation system", *Eng. Struct.*, **28**(1), 72-83. <https://doi.org/10.1016/j.engstruct.2005.07.003>.
- Uniform Building Code (1997), *Structural Engineering Design Provisions, California, International Conference of Building Officials*.
- Varnava, V. and Komodromos, P. (2013), "Assessing the effect of inherent nonlinearities in the analysis and design of a low-rise base isolated steel building", *Earthq. Struct.*, **5**(5), 499-526. <http://dx.doi.org/10.12989/eas.2013.5.5.499>.
- Zhang S. and Wang G. (2013), "Effects of near-fault and far-fault ground motions on nonlinear dynamic response and seismic damage of concrete gravity dams", *Soil Dyn. Earthq. Eng.*, **53**, 217-229. <https://doi.org/10.1016/j.soildyn.2013.07.014>.

AT